AD-A147 307 C2 SUB N (OPTICAL) STUDIES IN THE FREE ATMOSPHERE BASED ON RAWINSONDE DATA(U) AIR FORCE GEOPHYSICS LAB HANSCOM AFB MA E A MURPHY ET AL. 26 APR 84 AFGL-TR-84-0135 1/1

UNCLASSIFIED F/G 4/1 NL

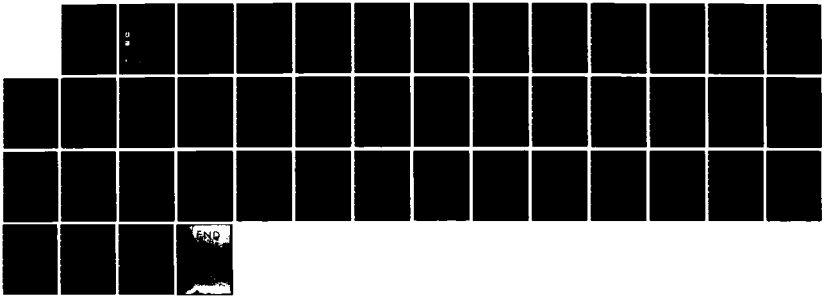

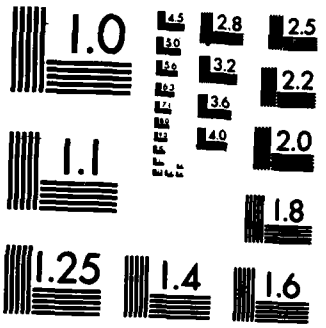
1.0
1.1
1.25
1.4
1.6
1.8
2.0
2.2
2.5
2.8
3.2
3.6
4.0
4.5
5.0
5.6
6.3
7.1

AFGL-TR-84-0135
ENVIRONMENTAL RESEARCH PAPERS, NO. 878

(12)

C_n^2 (Optical) Studies in the Free Atmosphere Based on Rawinsonde Data

EDMUND A. MURPHY
FRANK P. BATTLES
KATHRYN G. SCHARR
JOHN R. McCORMACK

26 April 1984

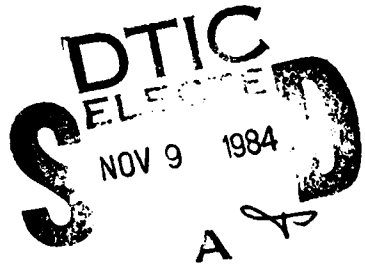

OPTICAL PHYSICS DIVISION PROJECT 7670
AIR FORCE GEOPHYSICS LABORATORY
HANSCOM AFB, MA 01731

This report has been reviewed by the ESD Public Affairs Office (PA) and is releasable to the National Technical Information Service (NTIS).

This technical report has been reviewed and is approved for publication.

FOR THE COMMANDER

ROBERT W. FENN
Branch Chief

JOHN S. GARING
Division Director

Qualified requestors may obtain additional copies from the Defense Technical Information Center.

If your address has changed, or if you wish to be removed from the mailing list, or if the addressee is no longer employed by your organization, please notify AFGL/DAA, Hanscom AFB, MA 01731. This will assist us in maintaining a current mailing list.

Do not return copies of this report unless contractual obligation or notices on a specific document requires that it be returned.

Unclassified

SECURITY CLASSIFICATION OF THIS PAGE

REPORT DOCUMENTATION PAGE

1a. REPORT SECURITY CLASSIFICATION Unclassified	1b. RESTRICTIVE MARKINGS
2a. SECURITY CLASSIFICATION AUTHORITY	3. DISTRIBUTION/AVAILABILITY OF REPORT Approved for public release; distribution unlimited.
2b. DECLASSIFICATION/DOWNGRADING SCHEDULE	
4. PERFORMING ORGANIZATION REPORT NUMBER(S) AFGL-TR-84-0135 ERP, No. 878	5. MONITORING ORGANIZATION REPORT NUMBER(S)
6a. NAME OF PERFORMING ORGANIZATION Air Force Geophysics Laboratory 6b. OFFICE SYMBOL (If applicable) OPA	7a. NAME OF MONITORING ORGANIZATION
6c. ADDRESS (City, State and ZIP Code) Hanscom AFB Massachusetts 01731	7b. ADDRESS (City, State and ZIP Code)
8a. NAME OF FUNDING/SPONSORING ORGANIZATION 8b. OFFICE SYMBOL (If applicable)	9. PROCUREMENT INSTRUMENT IDENTIFICATION NUMBER
8c. ADDRESS (City, State and ZIP Code)	10. SOURCE OF FUNDING NOS. PROGRAM ELEMENT NO. 62101F; PROJECT NO. 7670; TASK NO. 15; WORK UNIT NO. 08
11. TITLE (Include Security Classification) C_n^2 (Optical) Studies in the Free Atmosphere Based on Rawinsonde Data	
12. PERSONAL AUTHOR(S) Edmund A. Murphy, Frank P. Battles*, Kathryn G. Scharr*, and John R. McCormack*	
13a. TYPE OF REPORT Scientific - Final 13b. TIME COVERED FROM 10/1/82 TO 9/30/84	14. DATE OF REPORT (Yr., Mo., Day) 1984 April 26 15. PAGE COUNT 42
16. SUPPLEMENTARY NOTATION * Bedford Research, Bedford, MA 01730 (F. P. Battles also professor, Massachusetts Maritime Academy)	
17. COSATI CODES FIELD / GROUP / SUB. GR.	18. SUBJECT TERMS (Continue on reverse if necessary and identify by block number) Index of refraction; Structure parameter; Optical turbulence; Atmospheric optical turbulence; Atmospheric optical effects

19. ABSTRACT (Continue on reverse if necessary and identify by block number)

Rawinsonde data from several locations in the United States are used to obtain free atmosphere estimates of C_n^2 (optical), the index of refraction structure parameter. Wind and temperature data are used to calculate N, the square of the Brunt-Väisällä frequency, S, the wind shear squared term, and the Richardson number at kilometer intervals from 1 km to 25 km. These quantities are inputs to the Van Zandt model to determine C_n^2. Also, the rms wind speed (u), obtained from the rawinsonde data, is used as input to the Hufnagel model to obtain C_n^2. Aspects of the C_n^2 models are discussed and comparisons are made using model results and C_n^2 radar measurements. Statistical analysis of results indicate significant differences in median C_n^2 distributions for both season and latitude. Coherence lengths (r_o) for plane wave propagation down through the atmosphere are estimated and dropoff rates of C_n^2 (in dB/km) are calculated from 15 km to 25 km.

20. DISTRIBUTION/AVAILABILITY OF ABSTRACT UNCLASSIFIED/UNLIMITED ☒ SAME AS RPT. ☐ DTIC USERS ☐	21. ABSTRACT SECURITY CLASSIFICATION Unclassified
22a. NAME OF RESPONSIBLE INDIVIDUAL Edmund A. Murphy	22b. TELEPHONE NUMBER (Include Area Code) (617) 861-3016 22c. OFFICE SYMBOL OPA

DD FORM 1473, 83 APR EDITION OF 1 JAN 73 IS OBSOLETE.

Unclassified

SECURITY CLASSIFICATION OF THIS PAGE

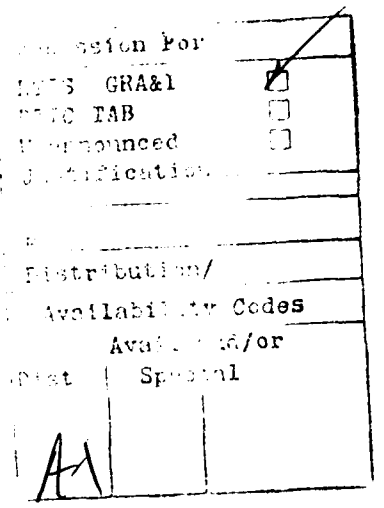

Contents

Illustrations

Illustrations

Tables

C_n^2 (Optical) Studies in the Free Atmosphere Based on Rawinsonde Data

1. INTRODUCTION

Atmospheric turbulence has long been known by astronomers to affect light radiation passage through the atmosphere. For optical systems, the single most important parameter describing the turbulent atmosphere is C_n^2 (the index of refraction structure parameter). This parameter is also related to the temperature structure parameter (C_T^2), which is a variable that is easier to measure than C_n^2. C_n^2 can be obtained from measurements of C_T^2 using the simplifying assumption that the index of refraction fluctuation depends only on the fluctuations in temperature. In this case the only other variables required are the temperature and pressure. The temperature structure function can be obtained by using thermosondes that require two similar probes spaced a distance r apart for measuring temperature. Thermosonde measurements can be obtained "in situ" in the free atmosphere using aircraft and balloons. Remote sensing techniques for indirect measurements of C_n^2 include stellar scintillometers and incoherent radars. The scintillometers measure the fluctuations in starlight caused by the atmosphere for different spatial wavelengths and use weighting functions for altitude resolution. Radars detect returns from fluctuations in the refractive index of the atmosphere caused by turbulence. The reader is referred to a section in the Infrared Handbook

(Received for publication 19 April 1984)

entitled "Propagation Through Atmospheric Turbulence"[1] for more detailed background information on C_n^2 and other optical parameters. This section presents excellent practical applications for obtaining estimates of C_n^2 and also contains a large number of references on the subject. Also, Good et al[2] contains comparisons of recent scintillometer and radar measurements of C_n^2.

In this paper several models are reviewed and the Hufnagel model[3] is compared with the Van Zandt model.[4,5] Both models use rawinsonde thermodynamic data to derive estimates of C_n^2. The rawinsonde data base has been previously used by Murphy et al,[6] and Murphy and Scharr[7] to model Richardson-number (Ri)-inferred estimates of the likelihood of occurrence of turbulence in the lower atmosphere. The same derived quantities used in that study, namely the winds, N (the square of the Brunt-Väisällä frequency, S (the vertical shear of horizontal winds squared term), and the ratio N/S (the Richardson number) are required and used as inputs to the Hufnagel and Van Zandt models to obtain C_n^2 estimates. Also, drop-off rates of C_n^2 and coherence lengths (r_o) are determined and the C_n^2 drop-off rates are compared to those obtained from radar measurements.

The twice daily rawinsonde balloon measurements of wind and temperature at each of many locations (81 locations in the continental United States) are fit using a function that closely approximates a linear fit from point to point of the original data. The temperature, the temperature gradient, and the wind component gradients are determined from the fitting function equation by computer at each kilometer level from 1 km to 25 km. Daily values of the stability term, shear term, and Richardson number are accumulated in bins at each km level to provide seasonal statistics (~ 180 values/season). There are two reasons for not using data below 1 km. The first is that the stations used in this study had varying site elevations that precluded obtaining a good statistical sample for heights below 1 km. Also, data were not used below 1 km since we were inclined to limit this study to that region regarded as above the "boundary layer" which is generally defined to be above approximately 1 km. The upper level of 25 km was chosen since this criterion provided a near maximum of 100 samples per season for all stations at this level. Balloon bursts above this level greatly reduce the sample size.

The results presented here represent only a first step in developing a climatology of C_n^2 for optical effects. C_n^2 estimates are obtained only above the first kilometer and for dry conditions. For optical effects then, we are only interested in the optical refractivity, C_n^2(opt), which is the radio refractivity less the humidity term. Also, results from models should be compared with actual C_n^2 measurements to determine differences which have to be accounted for by improvements in the models.

(Due to the large number of references cited above, they will not be listed here. See References, page 37.)

2. A SURVEY OF SEVERAL MODELS FOR C_n^2

In most optical applications, one must integrate the product of C_n^2 and some function of distance along the optical path.[1] For other than horizontal propagation, we need to be able to model the height dependence of C_n^2 since it is highly unlikely that values will be directly available. Furthermore, to construct climatologies of C_n^2 from rawinsonde profiles of wind velocities, temperature, and pressure, a theoretical model is needed. In this section we discuss several such models.

An extremely simple model for C_n^2 is:[1]

$$C_n^2 = \begin{cases} \dfrac{1.5 \times 10^{-16}}{\hat{z}} & \text{below 20 km above sea level} \\ 0 & \text{above 20 km above sea level} \end{cases} \quad (1)$$

where $\hat{z}$ (in km) is altitude above local ground. The advantage of this model is its simplicity, but it cannot be expected to yield anything other than qualitative results when used to calculate the effects of turbulence on optical beams.

Hufnagel[1,3] used

$$C_n^2 = 2.7 \times 10^{-16} [3\, u^2 (z/10)^{10} e^{-z} + e^{-z/1.5}] . \quad (2)$$

In this empirical model, z is the elevation above sea level in km, and u is the rms wind speed (in m/sec) in the range from z = 5 km to z = 20 km, that is,

$$u^2 = 1/15 \int_5^{20} u^2(z)\, dz \quad (3)$$

where u(z) is the wind speed at altitude z. This model was constructed to best fit measurements of C_n^2 from z = 24 km down to the first strong inversion layer and so this is its expected range of validity. Use of the appropriate value of u^2 obtained from rawinsonde data, brings this model to within a factor of 2 of the median values of C_n^2 obtained by other methods.[8,9,10] Although this model cannot be

---

8. Balsley, B. B., and Peterson, V. L. (1981) Doppler radar measurements of clear air turbulence at 1290 MHz, J. Appl. Meteorol., 20:266-274.
9. Barletti, R., Cappatelli, G., Paterno, L., Righini, A., and Speroni, M. (1976) Mean vertical profile of atmospheric turbulence relevant for astronomical seeing, J. Opt. Soc. Am., 66:1380-1383.
10. Nastrom, G. D., Gage, K. S., and Balsley, B. B. (1982) Variability of C_n^2 at Poker Flat, Alaska, from mesosphere, stratosphere and troposphere (MST) Doppler radar observations, Opt. Eng., 21:347-351.

expected to agree with a single set of measurements of C_n^2, it can be modified to yield typical fine structure patterns.[3] We note that for z and u^2 large enough, this model predicts that C_n^2 is directly proportional to u^2.

Two recent theoretical models have been developed by Van Zandt et al[4,5] to allow calculations of C_n^2 from routine rawinsonde data. These models are based on the empirical fact that turbulence occurs in thin layers and on the theoretical work of Tatarskii[11] who has shown that in a homogeneous isotropic turbulent layer

$$C_n^2 = a^2 \alpha' L^{4/3} M^2 , \tag{4}$$

where a^2 is a constant approximately equal to 2.8, α' is the ratio of eddy diffusivities, which is assumed to be unity, L is the outer scale length of the turbulence spectrum, and M is the vertical gradient of the refractive index (neglecting humidity). M is given by:

$$M = -77.6 \times 10^{-6} P/T \frac{\partial}{\partial z} \ln \theta , \tag{5}$$

where P is the atmospheric pressure in millibars, T is the absolute temperature and θ is the potential temperature.

It is important to emphasize that this relationship for C_n^2 holds only in the presence of shear turbulence. This is defined to occur when the Richardson number, Ri, is equal to or less than one-quarter, where

$$Ri = N/S \tag{6}$$

and $N = g \frac{\partial}{\partial z} \ln \theta$, $g = 9.8\ m/sec^2$, and $S = (\partial V/\partial z)^2$. N is the static stability term and S is the shear parameter. (Note: this notation has by no means been standardized in the literature and care must be used in comparing formulas from different sources. We use N for the square of the Brunt-Väisällä frequency and S for the square of the vertical velocity gradient.) On substitution we obtain

$$C_n^2 = 1.76 \times 10^{-10} (P/T)^2 N^2 L^{4/3}, \text{ if } Ri = N/S \leq 1/4 . \tag{7}$$

---

11. Tatarskii, V. I. (1971) The Effects of the Turbulent Atmosphere on Wave Propagation, U.S. Dept. of Commerce, National Technical Information Service, Springfield, VA, pp. 74-76.

This result shows the basic problem in using rawinsonde data to calculate C_n^2. What is obtained from this data base are values of N and S averaged over hundreds of meters, whereas the use of the above equation requires the use of local values of N and S only for $N/S \leqq 1/4$. In the first model of Van Zandt et al,[4] it is assumed that $\bar{C}_n^2$, the average value of C_n^2 across an observed layer of atmosphere, can be calculated from $\bar{C}_n^2 = C_n^2 F$ where C_n^2 is calculated using averaged values of P, T, and N for the given layer and F is the fraction of the layer that is turbulent. L is treated as an adjustable parameter. F is calculated by assuming that the probability distribution for the velocity shear is normal, with the mean value obtained from rawinsonde data, and has a standard deviation of 0.010 sec^{-1} in the troposphere and 0.015 sec^{-1} in the stratosphere. F can then be calculated by integrating this distribution over those values for which $Ri \leqq 1/4$. With a choice of L = 10 m, good agreement between $\bar{C}_n^2$ and an average of C_n^2 from radar data is obtained.

The above model has been improved recently by Van Zandt et al[5] by including fine structure in the static stability, N, in addition to the velocity shear term, S. Furthermore, the parameter L is treated as a variable layer thickness. It is assumed that

$$\bar{C}_n^2 = \int_0^\infty dL \iint_{R_i \leqq 1/4} dS\, dN\, p^t(L, S, N)\, C_n^2 \tag{8}$$

where $p^t(L, S, N)\, dL\, dS\, dN$ is the probability that a point in a turbulent layer has values of L, S and N lying between L and L + dL, S and S + dS and N and N + dN. It is assumed within the limits of integration that $p^t(L, S, N) = 0$ if $Ri > 1/4$. Since $p^t(L, S, N)$ is not known precisely, certain assumptions are required. It is assumed that

$$p^t(L, S, N) = p^t(L)\, p^t(S)\, p^t(N)\,, \tag{9}$$

that is, the marginal distributions are independent and further that

$$p^t(X) = p^0(X)\,, \tag{10}$$

where the superscript of zero indicates non-turbulent conditions and X represents any of the three variables. This means we are assuming that the probability distributions for the individual variables are unchanged as we change from turbulent to non-turbulent conditions. $p^0(L)$, however, must be related to the probability that a point is in a layer of thickness L whether that layer is turbulent or not. The individual distributions assumed are as follows:

$$\text{(a)} \quad p^0(S) = \exp[-(S + \overline{S})/2\sigma_S^2]\ I_0[(S \times \overline{S})^{0.5}/\sigma_S^2]/2\sigma_S^2 . \tag{11}$$

This is the Rice-Nakagami distribution. $\overline{S}$ can be calculated from the rawinsonde data and σ_S is the standard deviation of either component of $\partial V/\partial z$. For computational purposes, the Rice-Nakagami distribution is rewritten in the form

$$P^0(S) = \exp\left[\frac{2(S\,\overline{S})^{0.5} - (S + \overline{S})}{2\,\sigma_S^2}\right] \exp(-x)\, I_0(x)/2\sigma_S^2 \tag{12}$$

where

$$x = (S\,\overline{S})^{0.5}/\sigma_S^2 . \tag{13}$$

Based on Essenwanger's empirical work[12] on standard deviations for wind shears, it is assumed that

$$\sigma_S(S^{-1}) = a_S(S^{-1})\,L^{-\alpha_s} \tag{14}$$

with a_S chosen as 2×10^{-2} sec^{-1} and 3×10^{-2} sec^{-1} for the troposphere and stratosphere respectively and α_s chosen as 0.3. We note that with the choice of L = 10 m, this is consistent with the 1978 model[4] values of σ_S. I_0 is the modified Bessel function of the first kind.

$$\text{(b)} \quad \rho^0(N) = \exp[-(N - \overline{N})^2/2\sigma_N^2]/(2\pi)^{1/2}\ \sigma_N \tag{15}$$

where $\overline{N}$ is obtained from rawinsonde data and it is assumed that $\sigma_N = (\overline{N})^{1/2}\,\sigma_S$

$$\text{(c)} \quad \rho^0(L) = \exp(-L/\overline{L})\,[(L/\overline{L})\,(1/\overline{L})] . \tag{16}$$

The justification for this distribution is based on the likelihood of an exponential distribution of L with the factor $L/\overline{L}$ added to provide zero probability at zero length. $\overline{L}$ is chosen to best fit the radar data and again turns out to be 10 m.

These assumptions yield better agreement with radar results.

---

12. Essenwanger, O. (1963) On the derivation of frequency distributions of vector wind shear values for small shear intervals, Geophysica Pura e Applicata, 56:216-224.

In either of Van Zandt's models we can see the somewhat complicated dependence of C_n^2 on the Richardson number. As Ri decreases, the fraction of the observed layer that is mechanically turbulent increases, which of itself would cause C_n^2 to increase. On the other hand, if Ri decreases due to a decrease in N (the static stability) this would, of itself, cause C_n^2 to decrease since, from Tatarskii's basic result, we can see that C_n^2 is directly proportional to N^2.

The subroutine shown in Appendix A was used to implement Van Zandt's 1981 model, with two changes, suggested by Van Zandt, [13] from its original formulation. These are discussed below. The inputs to this subroutine are $\overline{N} > 0$ and $\overline{S}$ obtained from our fitting routine (Section 1) and the output is $\overline{C_n^2}/(P/T)^2$, which is then converted to C_n^2. If $\overline{N} < 0$, we assume that the entire region is turbulent and calculate $\overline{C_n^2}$ from Van Zandt's 1978 model with F = 1.

The form for a_S used has been changed from 2×10^{-2} sec^{-1} (troposphere) and 3×10^{-2} sec^{-1} (stratosphere) to $a_S = 0.2(\overline{N})^{1/4}$. This one-fourth power dependence on N is supported by some recent theoretical work of Weinstock. [14] The advantage of this form is that it provides a continuous variation of σ_S and does not require the location of the tropopause.

The distribution function $p^0(L)$ has been changed from $(L/\overline{L^2})\, e^{-L/\overline{L}}$ to a flat distribution. We assume $p^0(L)$ is 0.01 over the range of L values used in the integration. Detailed analysis of the contribution of different layer thicknesses to the total $\overline{C_n^2}$ value reveals that thick layers beyond 100 m contribute small amounts. This definition of L is used in the Van Zandt model[5] for ease of computation. The Tatarskii[11] definition of L is the outer scale length of isotropic turbulence. The definition of shear turbulence through the Richardson number criterion leads to a turbulence layer thickness, H, used to define the vertical gradients of potential temperature and horizontal winds. The relationship between outer scale length, L, and turbulent layer thickness, H, is not well defined. Experiments by Good et al[15] have indicated that above the boundary layer, the outer length scale is about 1/10 the turbulent layer thickness. If this is incorporated into the Van Zandt Model, [5] then substituting L = H/10 into Eq. (7).

$$C_n^2 = 8.2 \times 10^{-12} (P/T)^2 N^2 H^{4/3} \tag{17}$$

with N^2 and Ri evaluated on the basis of turbulent layer thickness H. With this modification, it will be necessary to increase the probability of turbulent layer

13. Van Zandt, T.E. (1983) private communication.

14. Weinstock, J. (1980) Vertical wind shears, turbulence, and non-turbulence in the troposphere and stratosphere, Geophys. Res. Letts., 7:749-752.

15. Good, R.E., Quesada, A.F., Brown, J.H., and Dewan, E.M. (1984) Probability distribution of turbulence layer thickness in the stratosphere, J. Geophys. Res., to be published.

occurrence to match observed optical turbulence values. The effect is to change constants but does not change the underlying relationship of C_n^2 to meteorological wind and temperature data.

3. STATISTICAL RESULTS FOR C_n^2 FROM VAN ZANDT'S MODEL

Our examination of the characteristics of the C_n^2 distribution included four stations: Barrow, Alaska (71° N), International Falls, Minnesota (48° N), Pt. Mugu, California (34° N), and Brownsville, Texas (25° N) for each season: winter, spring, summer, fall. Each season was defined using solstice and equinox dates:

Winter	-	December 21 through March 20,
Spring	-	March 21 through June 20,
Summer	-	June 21 through September 20,
Fall	-	September 21 through December 20.

C_n^2 median seasonal values were computed at altitudes ranging from 1 to 25 km using the N and S values determined from rawinsonde daily measurements.

A series of plots were drawn examining seasonal and latitudinal variations of C_n^2 as a function of altitude. Different combinations of stations and seasons were overlayed to examine the structure of the median C_n^2 values over 1 - 25 km. Figure 1 contains the two extremes in latitude for the winter, Brownsville, Tex., (25° 54' N) and Barrow, Alaska (71° 18' N). There are significant differences in the distribution of median C_n^2 values between 10 and 20 km. Although not as pronounced, the same structure was found between Pt. Mugu, Calif. (34° 6' N) and International Falls, Minn. (45° 34' N), which is shown in Figure 2. All four stations are plotted in Figure 3. As latitude increases, there is a distinct decrease in C_n^2 between 10 and 20 km. Examination of summer median C_n^2 latitudinal variations revealed only slight differences over the 1 - 25 km region (Figure 4). There was a shift, however, in each distribution in the approximate height range between 12 and 15 km. This may be due to the jet stream.

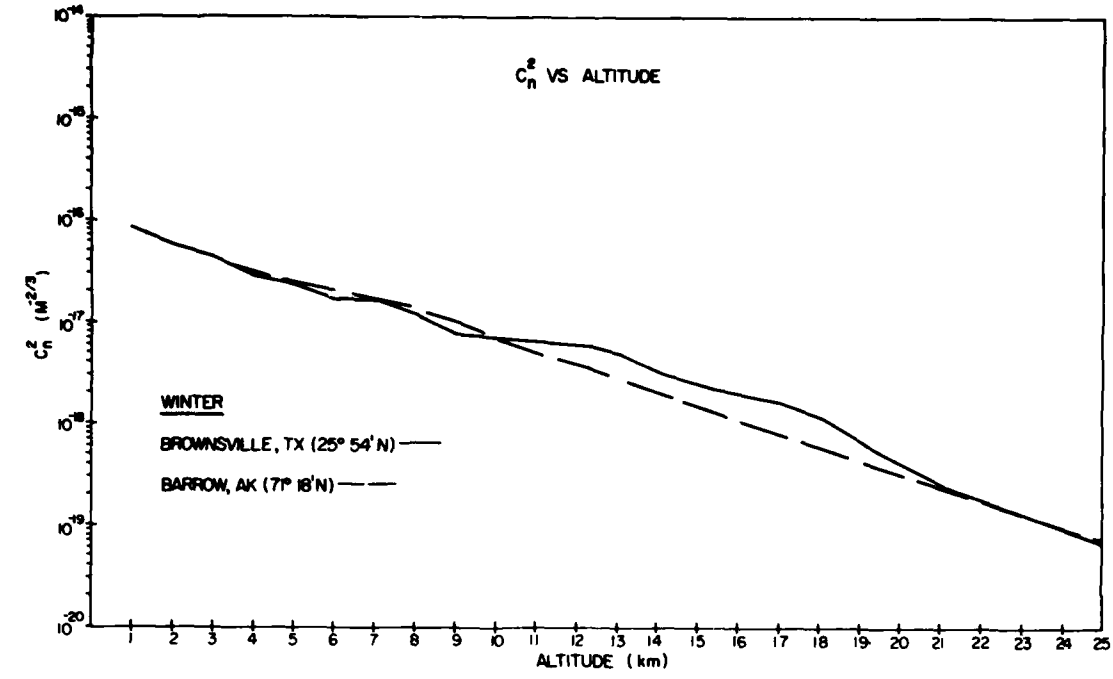

Figure 1. C_n^2 vs Altitude: Winter 1974, Brownsville, Tex. and Barrow, Alaska

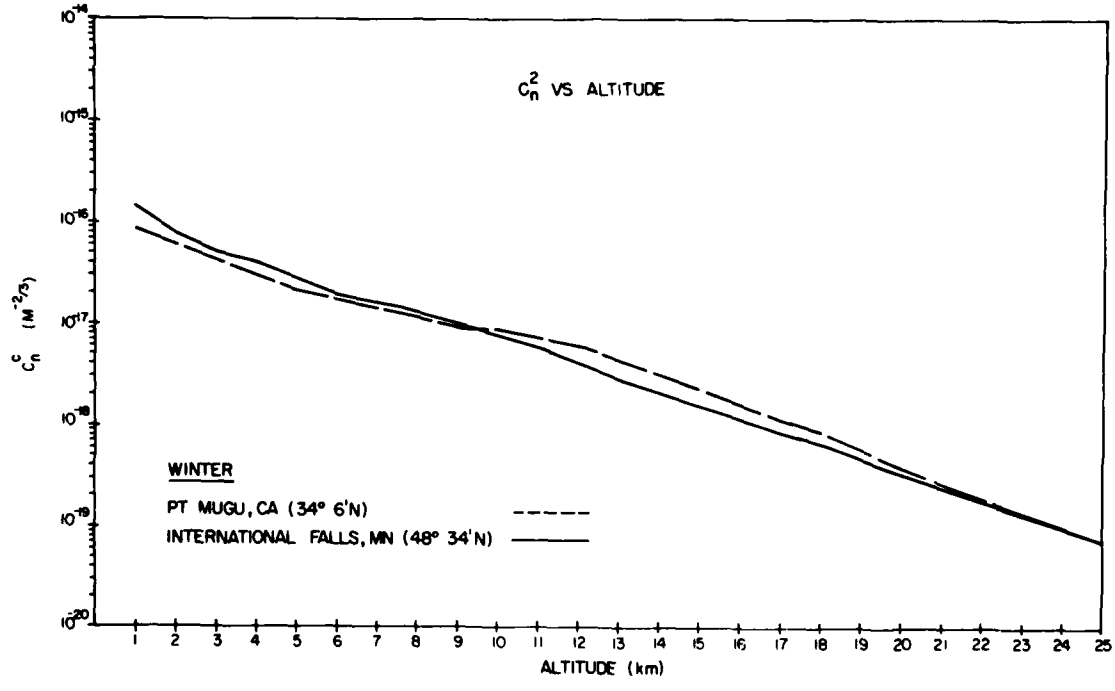

Figure 2. C_n^2 vs Altitude: Winter 1974, Pt. Mugu, Calif. and International Falls, Minn.

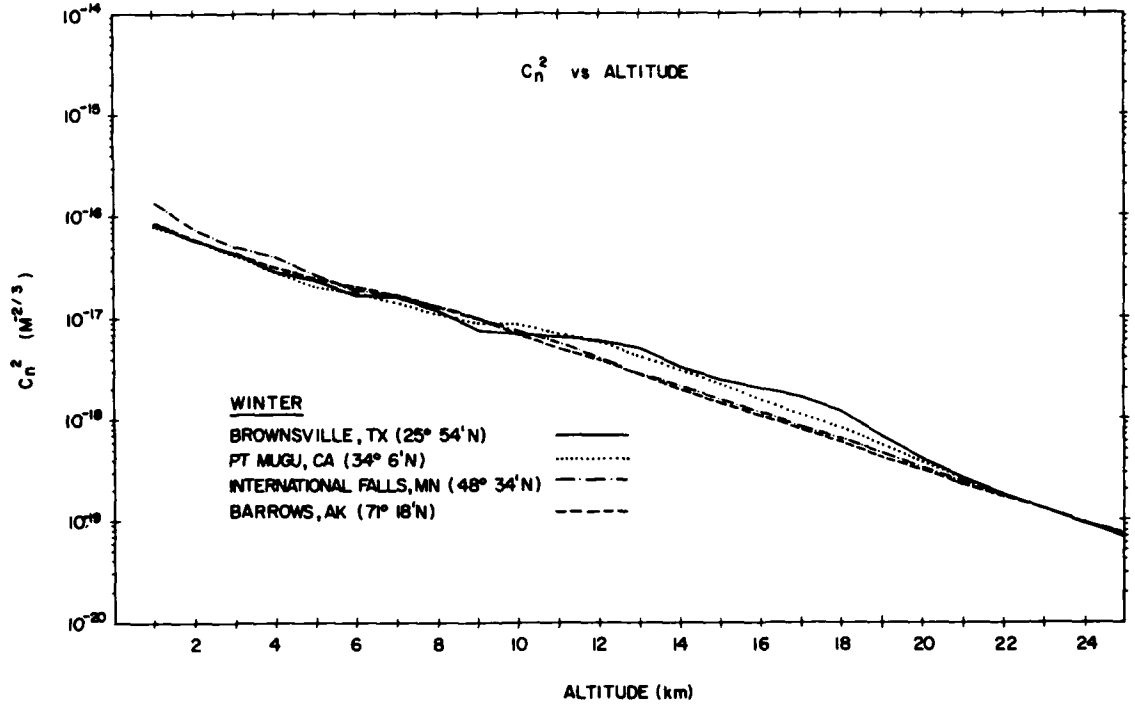

Figure 3. C_n^2 vs Altitude: Winter 1974, Brownsville, Tex.; Pt. Mugu, Calif.; International Falls, Minn.; and Barrow, Alaska

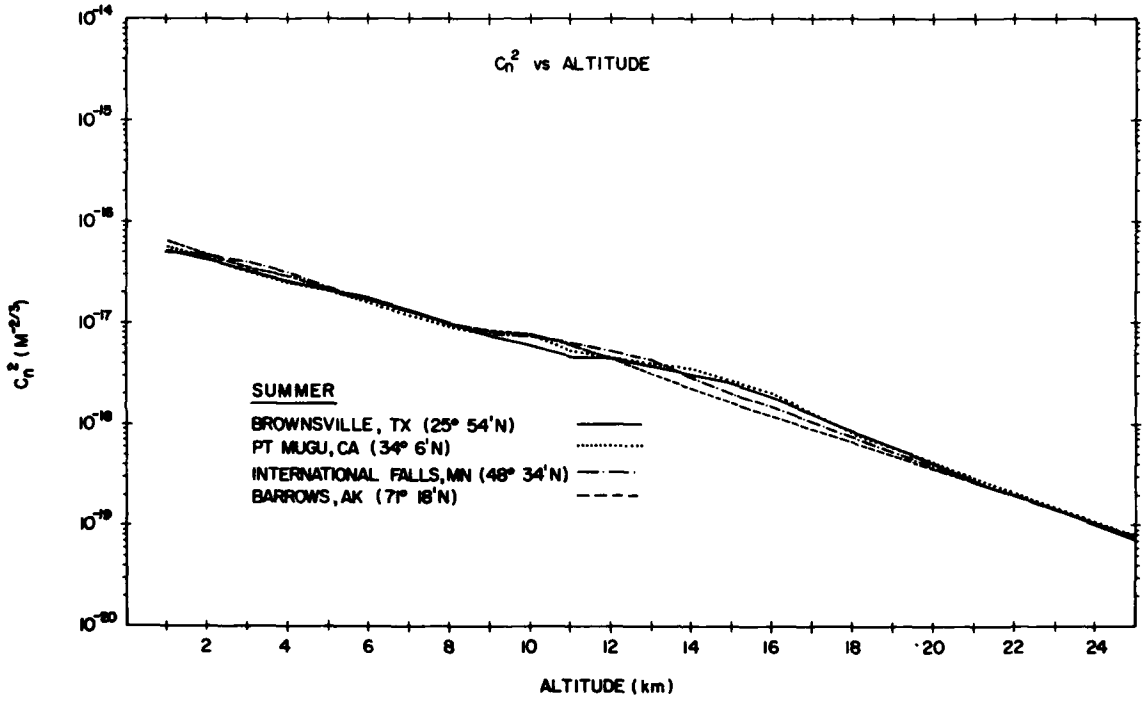

Figure 4. C_n^2 vs Altitude: Summer 1974, Brownsville, Tex.; Pt. Mugu, Calif.; International Falls, Minn.; and Barrow, Alaska

A comparison was made of winter and summer median C_n^2 values for each of the four stations. The winter and summer plots for Barrow, Alaska are presented in Figure 5. The winter curve was fairly linear from 1 to 25 km, while the summer curve had an inflection point around 10 km. International Falls, Minn. (Figure 6) and Pt. Mugu, Calif. (Figure 7) demonstrated a similar trend with inflection points at 10 and 13 km respectively. The graph of Brownsville, Tex. (Figure 8) did not reveal the same structure as the others.

We were interested in seasonal and latitudinal variations of C_n^2 for each of the stations mentioned above. A non-parametric test was selected to measure the distributional differences between the four groups. This is called a "median test"[16] because the data from each group are arranged from the lowest to highest values and each value is then compared with the median of the combined groups. If the four groups are in fact from the same distribution, the number of values above and below the overall median should be about the same. The chi-square statistic measures the degree to which each group deviates from the expected combined distribution. A contingency table is then arranged and analyzed using a chi-square (χ^2) statistic having three degrees of freedom (number of groups minus 1). The hypothesis of identical distributions is rejected if the observed χ^2 is significantly large.

There was no significance found in accepting the hypothesis of identical distributions in examining latitudinal variations from station to station for each season. Each of the altitude levels from 1 to 25 km were examined separately (Table 1). A significantly large χ^2 statistic at the 5 percent level of significance was greater than χ^2 critical = 7.18. As is apparent from Table 1, random altitude levels demonstrate similar distributional characteristics; there is no apparent physical reason, however, why these exist. Therefore we can conclude that there are distinct differences in the distributions of the four stations, having differing latitudes, over the four seasons defined above.

In the examinations of seasonal variations, each station was tested for differences season to season at each kilometer level from 1 to 25 km using the test previously discussed. A similar phenomenon was found as with the latitudinal variation analysis (Table 2). There were significant differences season to season throughout each altitude bin from 1 to 25 km.

16. Dixon, W.J., and Massey, F.J. (1969) An Introduction to Statistical Analysis McGraw-Hill, p. 351.

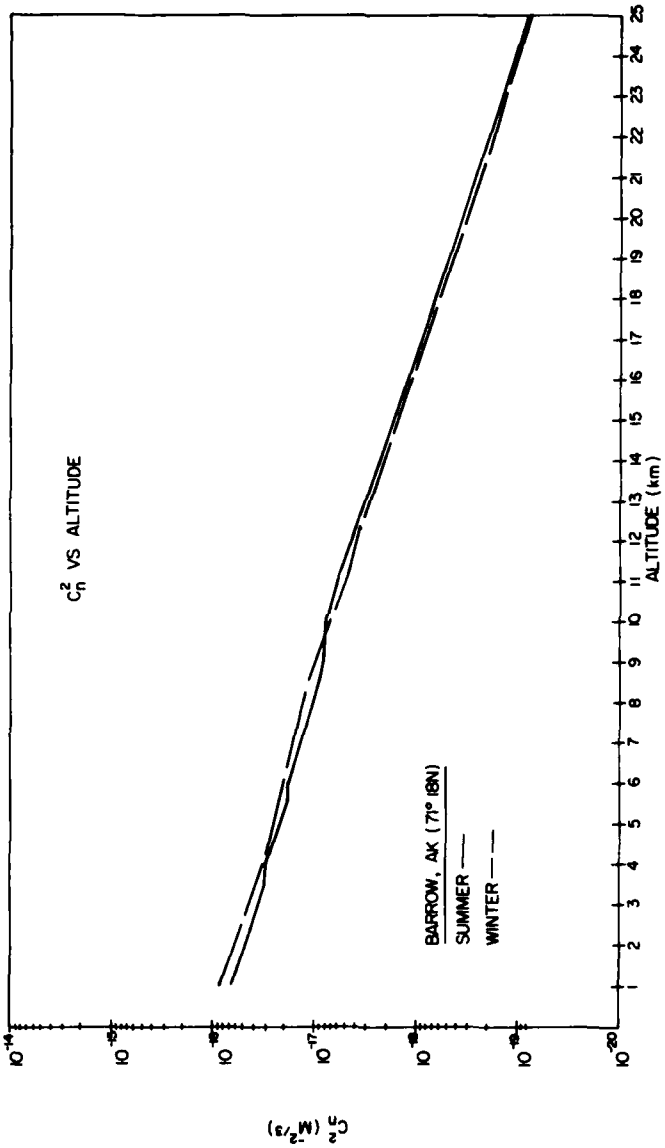

Figure 5. C_n^2 vs Altitude: Summer and Winter 1974, Barrow, Alaska

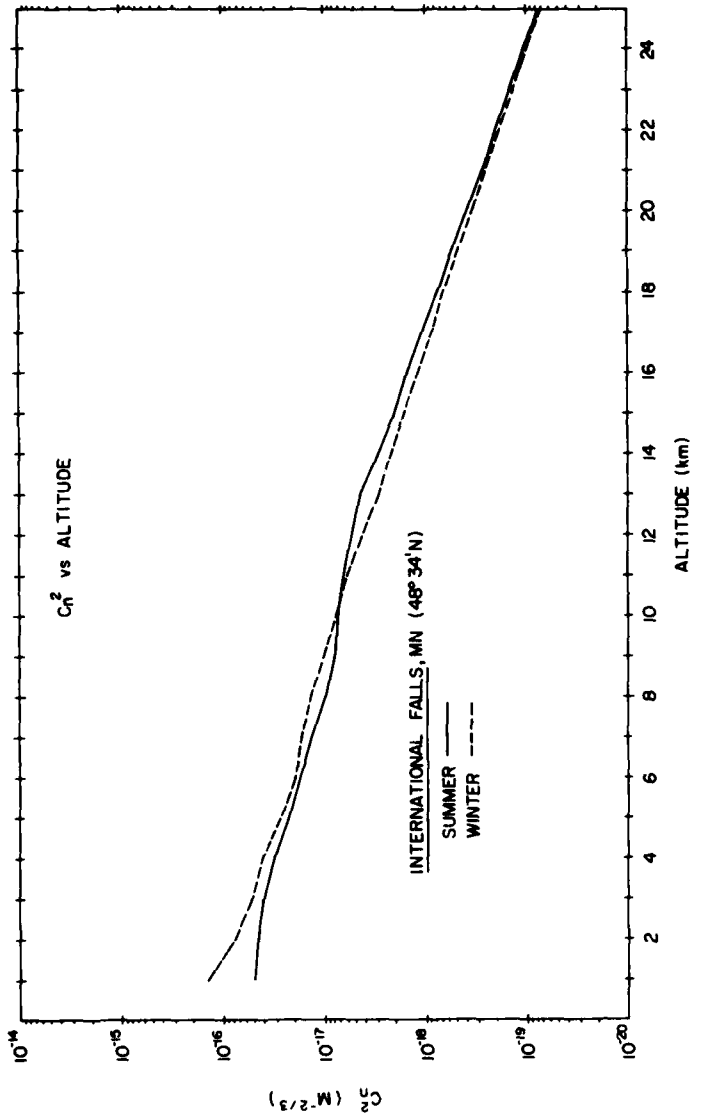

Figure 6. C_n^2 vs Altitude: Summer and Winter 1974, International Falls, Minn.

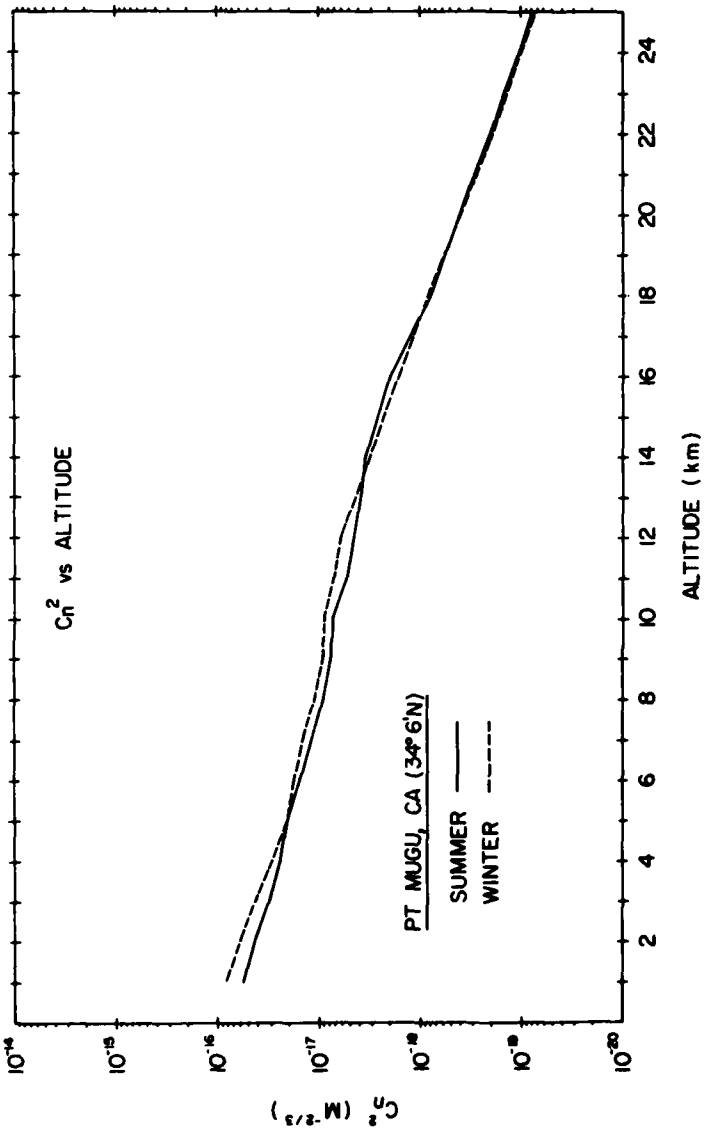

Figure 7. C_n^2 vs Altitude: Summer and Winter 1974, Pt. Mugu, Calif.

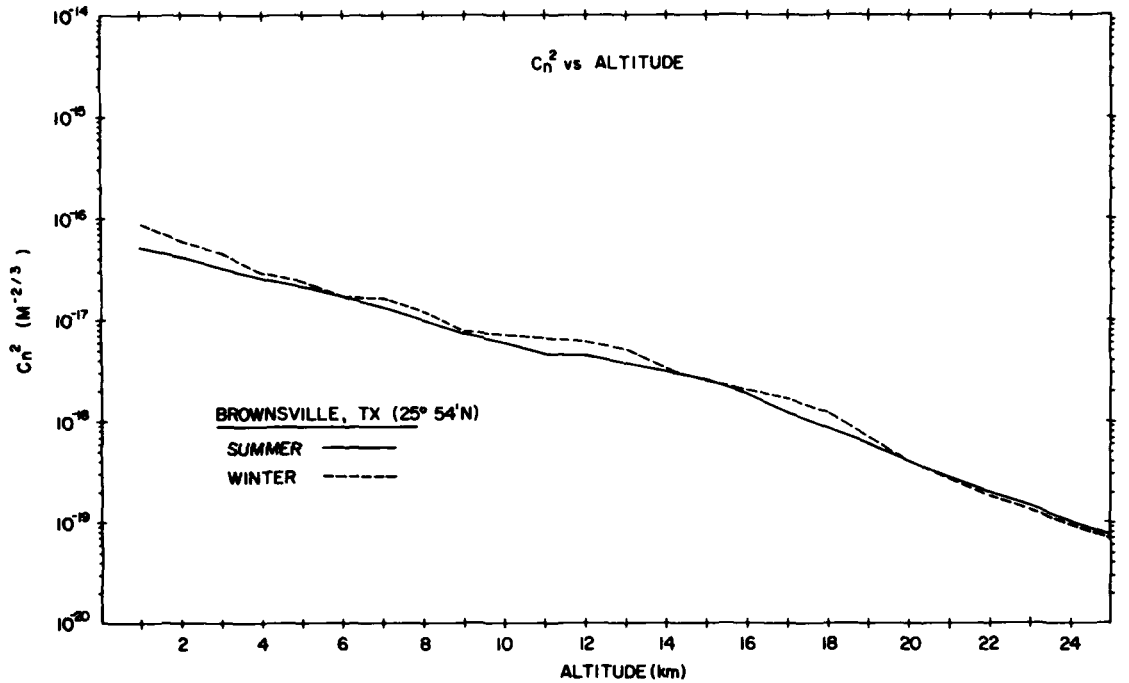

Figure 8. C_n^2 vs Altitude: Summer and Winter 1974, Brownsville, Tex.

Table 1. C_n^2 Median Test Results on Station-to-Station Differences

Altitude	Winter	Spring	Summer	Fall
1	16.77	13.68	22.77	6.93*
2	13.20	3.96*	13.96	4.75*
3	8.80	9.27	25.28	0.94*
4	26.75	12.11	52.09	2.73*
5	25.25	49.59	6.29*	23.47
6	12.69	39.42	11.78	13.13
7	6.59*	35.20	11.08	9.41
8	9.21	39.16	7.64*	18.59
9	9.50	28.38	9.63	15.41
10	18.83	28.20	22.60	7.41*
11	82.63	43.92	94.29	75.33
12	140.19	90.54	26.70	136.30
13	213.70	160.14	70.33	168.21
14	229.28	230.14	171.19	216.50
15	242.40	363.35	209.91	243.52
16	270.83	404.65	260.06	345.92
17	261.89	388.56	221.85	312.08
18	188.40	287.23	193.36	169.55
19	154.28	262.32	163.49	132.57
20	102.97	174.87	140.62	109.73
21	44.71	117.13	105.86	46.64
22	27.15	39.98	42.93	63.89
23	7.55*	20.66	7.49*	26.60
24	9.11	28.46	84.48	9.85
25	14.38	30.29	27.97	13.01

$\chi^2_{critical} = 7.81$, Degrees of Freedom = 3

*Indicates non-rejection of differing distributions

Table 2. C_n^2 Median Test Results on Season-to-Season Differences

Altitude	Barrow	International Falls	Pt. Mugu	Brownsville
1	26.71	67.24	16.89	47.17
2	46.73	28.65	13.05	47.57
3	31.15	16.66	29.78	28.55
4	8.27	13.75	31.29	18.08
5	21.64	20.22	4.03*	11.20
6	10.21	10.53	8.44	12.64
7	39.77	6.38*	9.94	18.21
8	44.38	31.73	7.01*	28.62
9	26.68	19.45	5.69*	29.31
10	9.82	4.97*	11.15	15.76
11	72.44	8.28	59.39	30.37
12	81.95	35.29	60.03	54.95
13	125.30	92.43	11.42	30.97
14	128.77	63.91	4.74*	26.59
15	188.14	74.44	19.93	18.22
16	207.15	118.09	45.32	28.90
17	182.60	105.92	8.41	78.08
18	141.02	74.05	6.61*	88.15
19	144.50	65.92	3.63*	34.73
20	188.07	94.95	23.59	4.49*
21	161.49	90.86	45.84	29.70
22	136.62	145.68	87.43	70.58
23	92.28	107.82	80.44	51.34
24	69.79	90.39	86.52	51.62
25	107.43	131.05	82.37	54.10

$\chi^2_{critical} = 7.18$, Degrees of Freedom = 3

* Indicates non-rejection of differing distributions

4. THE HIGH ALTITUDE DROP-OFF RATE FOR C_n^2

Balsley and Peterson[8] first observed and systematically studied the fact that above an altitude of about 10 km the graph of the logarithm of the median of C_n^2 versus altitude becomes approximately linear. The median values used were obtained from radar measurements of C_n^2 over a period of time ranging from a day to several weeks. A similar observation can be made from our results using Van Zandt's model (see Figures 1 to 8), although the linear region appears to begin closer to 15 km.

Defining the drop-off rate of C_n^2 in dB/km by

$$D\text{-}R = -10/(z_2 - z_1) \log [C_n^2(z_2)/C_n^2(z_1)] \tag{18}$$

where z_i is the elevation above mean sea level in kilometers, Balsley and Peterson then look at the variation of this parameter as a function of time and of latitude. They conclude that it is relatively independent of time and is a decreasing function of latitude. Based on their somewhat limited data they suggest that much more work needs to be done to clarify these conclusions. Clearly, if valid, they go a long way towards developing a climatology for C_n^2 in the upper atmosphere and provide a way of estimating average effects of the turbulent atmosphere at this level on optical beams. We have gone on to investigate this area extensively by use of Van Zandt's model of 1981.[5]

For stations of various latitudes and for each season we have fitted the median of the logarithm of C_n^2 versus z to a straight line for three intervals: (a) 10 to 20 km since this approximates the range used by Balsley and Peterson; (b) 15 to 25 km since this range appears to be the best straight line fit to the Van Zandt model; and (c) over the entire range from 10 to 25 km. Since the interval from 15 to 25 km consistently yielded the largest value of r^2, the square of the Pearson correlation coefficient, we have defined our drop-off rate for this interval. See Table 3 for typical results for the three altitude ranges listed above.

Table 3. Drop-Off Rate (in dB/km) of C_n^2 and Associated Square of Correlation Coefficient for Pt. Mugu, Calif., 1974, for Three Altitude Ranges

Range	Winter	Spring	Summer	Fall
10 - 20 km	1.38 (0.993)	1.29 (0.979)	1.24 (0.965)	1.35 (0.986)
15 - 25 km	1.52 (0.999)	1.54 (0.997)	1.54 (0.997)	1.53 (0.999)
10 - 25 km	1.45 (0.997)	1.41 (0.991)	1.37 (0.986)	1.43 (0.994)

We first calculated the drop-off rate for six stations of varying latitude for the four seasons. Our results are summarized in Table 4. We observe little seasonal variation, especially at high latitudes, which would support the hypothesis that this parameter, when averaged over a long enough time period, is constant. We can also see that it is a decreasing function of latitude but this effect is not as pronounced as it is in the radar results of Balsley and Peterson. This could be due to the fact that our averaging is over a much longer period of time, about 90 days for each value. In Figure 9, we have graphed these results (as well as two additional stations, at about 48° N latitude, see below) for the winter season along with the radar results. We chose winter because most of the radar results were for this season.

Table 4. Drop-Off Rate (in dB/km) of C_n^2 for Four Seasons at Various Latitudes, 1974

Station	Latitude	Winter	Spring	Summer	Fall
Barrow, Alaska	71° 28' N	1.30	1.30	1.31	1.32
International Falls, Minn.	48° 34' N	1.36	1.40	1.44	1.42
Chatham, Mass.	41° 40' N	1.49	1.54	1.52	1.48
Pt. Mugu, Calif.	34° 06' N	1.52	1.54	1.54	1.53
Brownsville, Tex.	25° 54' N	1.68	1.69	1.55	1.63
San Andres, Columbia	12° 35' N	1.71	1.58	1.59	1.69

Next, we calculated the season drop-off rates for three stations of nearly the same latitude but differing longitudes. These results are presented in Table 5. We observe little difference with changing longitude and, again, little seasonal variation.

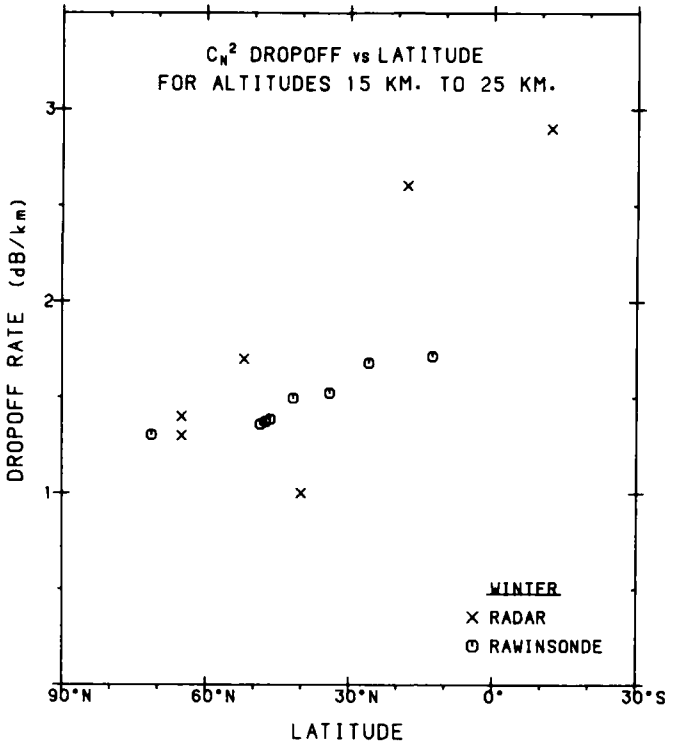

Figure 9. C_n^2 vs Latitude: Radar Results and Van Zandt Model Results From Rawinsonde Data for Winter 1974

Table 5. Drop-Off Rate (in dB/km) of C_n^2, 1974, for Four Seasons at Three Stations of Comparable Latitude

Station	Latitude	Longitude	Winter	Spring	Summer	Fall
Sault Sainte Marie, Mich.	46° 28' N	84° 22' W	1.37	1.43	1.46	1.43
Great Falls, Mont.	47° 29' N	111° 21' W	1.37	1.43	1.48	1.45
International Falls, Minn.	48° 34' N	93° 23' W	1.36	1.40	1.44	1.41

We can also determine the drop-off rate using a different approach. The models of Van Zandt[4,5] suggest that we can write

$$C_n^2 = (P/T)^2 G \tag{19}$$

where the function G depends on S, N and L (see Section 3). The function G includes, among other things, the fraction of an observed layer that is turbulent. Since P/T is proportional to the density, which we know decreases with increasing altitude, it is of interest to rewrite the above as

$$\log C_n^2 = \log (P/T)^2 + \log G \tag{20}$$

and calculate, from our data base, the density drop-off rate (in dB/km) of $(P/T)^2$; that is,

$$(D - R)_\rho = -10/(z_2 - z_1) \log[(P_2/T_2)^2/(P_1/T_1)^2] , \tag{21}$$

where P_i and T_i are the pressure and temperature at altitude z_i. This parameter can then be interpreted as that part of the drop-off rate in C_n^2 due only to decreasing density. This can also be interpreted as the drop-off for a constant C_T. For the usual exponential atmosphere with a constant density scale height, H_ρ, the drop-off rate is

$$(D - R)_\rho = 8.69/H_\rho . \tag{22}$$

The density scale height is related to the tabulated pressure scale height, H_p, as

$$H_\rho = H_p \Big/ \left[1 + H_p \frac{d}{dZ} \ln T \right] . \tag{23}$$

In the stratosphere where temperature change is small, $H_\rho = H_p \simeq 6.4$ km and the standard atmosphere drop-off rate is $(D - R)_\rho = 1.36$ dB/km.

After observing from our data base that $\log (P/T)^2$ is, to a good approximation, linear from z = 15 km to z = 25 km we evaluated the above for $z_1 = 15$ km and $z_2 = 25$ km for the same six stations used in Table 4 for each season. Since very little seasonal variation was found, in Table 6, we present just the average values for 1974. For comparison we have also provided the average value of the drop-off rate in C_n^2 for 1 -4 in Table 6. This table demonstrates that the two drop-off rates are quite close, differing by less than 1 percent at 71° N and by about 7.5 percent at 12° N, which suggests that the primary cause of the drop-off rate of C_n^2 is the fact that density decreases with elevation. We further note a decrease in the drop-off rate of $(P/T)^2$ with increasing latitude.

Table 6. Drop-Off Rate (in dB/km) of $(P/T)^2$ and C_n^2 for Various Latitudes, 1974

Station	Latitude	Drop-Off $(P/T)^2$	Drop-Off C_n^2
Barrow, Alaska	71° 28' N	1.30	1.31
International Falls, Minn.	48° 34' N	1.37	1.41
Chatham, Mass.	41° 40' N	1.40	1.51
Pt. Mugu, Calif.	34° 06' N	1.44	1.53
Brownsville, Tex.	25° 59' N	1.49	1.64
San Andres, Columbia	12° 35' N	1.52	1.64

5. TRANSVERSE COHERENCE LENGTH

The transverse coherence length, r_o, is a measure of the distortion of an optical wavefront by atmospheric turbulence. Coherence length is related to seven specific optical properties of a beam.[17] Over a circle of diameter r_o, wavefront distortion has an rms value of almost exactly 1 radian. The coherence length is given by the expression

$$r_o = 2.1\,(1.46\,k^2\,I)^{-3/5} \tag{24}$$

where k is the wavenumber, which is assumed for our calculations to be at the center of the optical band, $\lambda = 500$ nm. $I = \int C_n^2(z)\,Q(z)\,dz$ where $Q(z)$ is a function that depends on the nature of the optical source. For an infinite plane wave source, $Q(z) = 1$. This type of source is assumed throughout; then in order to calculate r_o for vertical propagation through the atmosphere we need to evaluate

$$I = \int_{z_o}^{\infty} C_n^2(z)\,dz \tag{25}$$

where z_o is the appropriate altitude.

17. Fried, D. L., and Meyers, G. E. (1974) Evaluation of r_o for propagation down through the atmosphere, Appl. Opt., 13:2620-2622.

To become familiar with the order of magnitude of the quantities involved, we refer to the work of Gracheva and Gurvich[18] who have evaluated this integral and then r_o under the extremes of strong and weak turbulence. For these cases they obtained an I of 1.37×10^{-10} $m^{1/3}$ and 5.79×10^{-13} $m^{1/3}$ respectively. Their respective coherence lengths were then 0.42 and 11.1 cm for a wavelength of 500 nm. They suggest using the geometric mean, r_o = 2.2 cm, as a representative value. By different methods, Walters and Kunkel[19] estimate the contribution to r_o of this integral above 1 km can be of the order of 10 to 20 percent. Thus, for r_o = 10 cm at 2km, the contribution above 1 km is between 1 and 2 cm. Although these values may be helpful in order of magnitude calculations, in many applications, a more accurate determination of r_o is required to reflect local conditions more correctly.

Although we expect the boundary layer to make the major contribution to this integral when z_0 lies in the layer,[19] the contribution of the free atmosphere is not negligible. We have followed two approaches in calculating this contribution; the first approach is based on Van Zandt's 1981 model[5] and the second is based on Hufnagel's model.[3]

By use of the $C_n^2(z)$ values obtained from Van Zandt's model (Section 3) at each km level from z = 1 km to z = 25 km, we have been able to approximate I by use of Simpson's Rule over the range from z_0 = 1 km to z_0 = 20 km. The lower value of z_0 is forced on us due to the lack of rawinsonde data below 1 km (Section 3). We stop at z_0 = 20 km since we must use z = 25 km, not infinity, as the upper limit of integration in I. One can estimate that this approximation is accurate to about 5 percent at z_0 = 20 km and increases rapidly in accuracy for z_0 < 20 km. Should we wish to extend the range above 20 km, we could easily do so using the appropriate drop-off rate (Section 4). This is probably not necessary since, at this high an altitude, r_0 is so large that diffraction effects dominate over optical turbulence effects in determining beam distortion. Some typical results from this calculation are shown in Figures 10 and 11.

---

18. Gracheva, M., and Gurvich, A. (1980) A simple model for calculation of turbulence noise in optical systems, Atmospheric and Oceanic Physics, 16:819-822.

19. Walters, D. L., and Kunkel, K. E. (1981) Atmospheric transfer function for desert and mountain locations: the atmospheric effects on r_o, J. Opt. Soc. Am., 71:397-405.

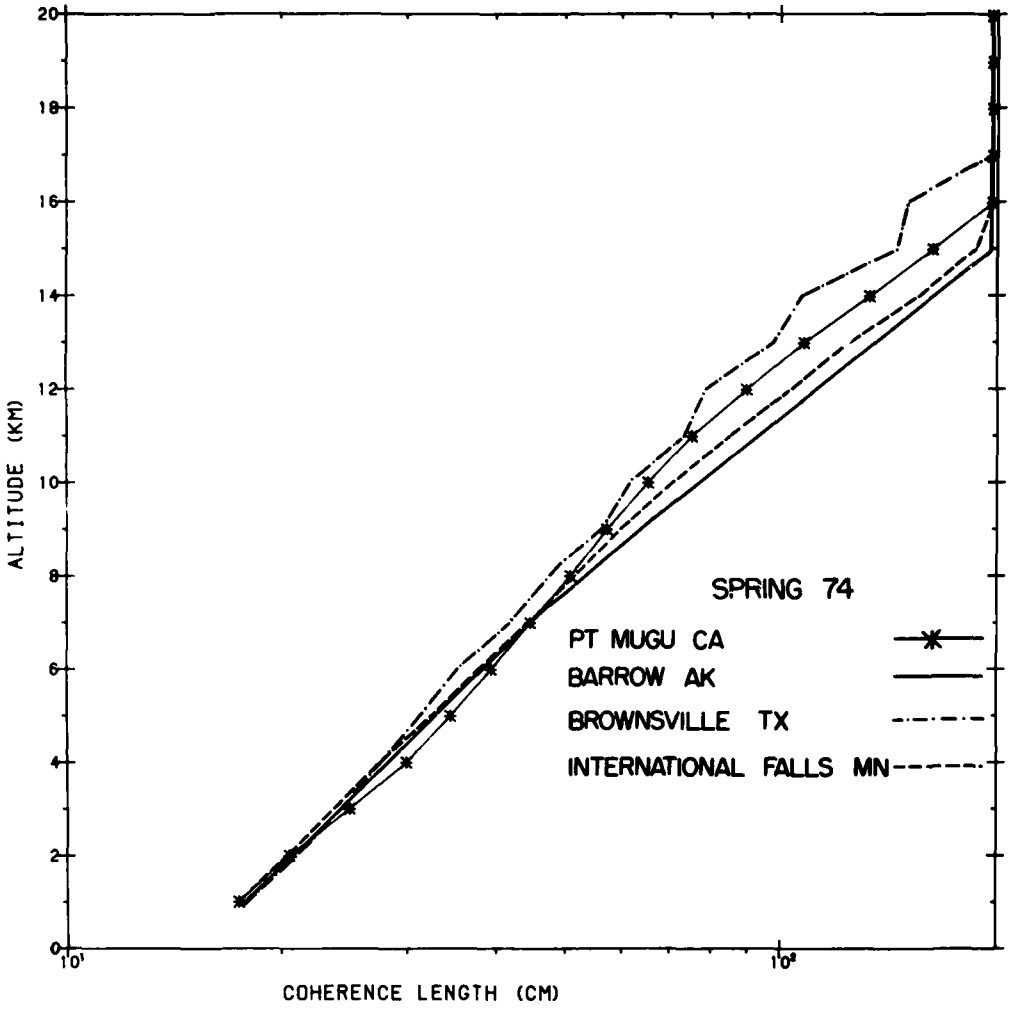

Figure 10. Coherence Length vs Altitude: Spring 1974, Pt. Mugu, Calif.; Barrow, Alaska; Brownsville, Tex.; and International Falls, Minn.

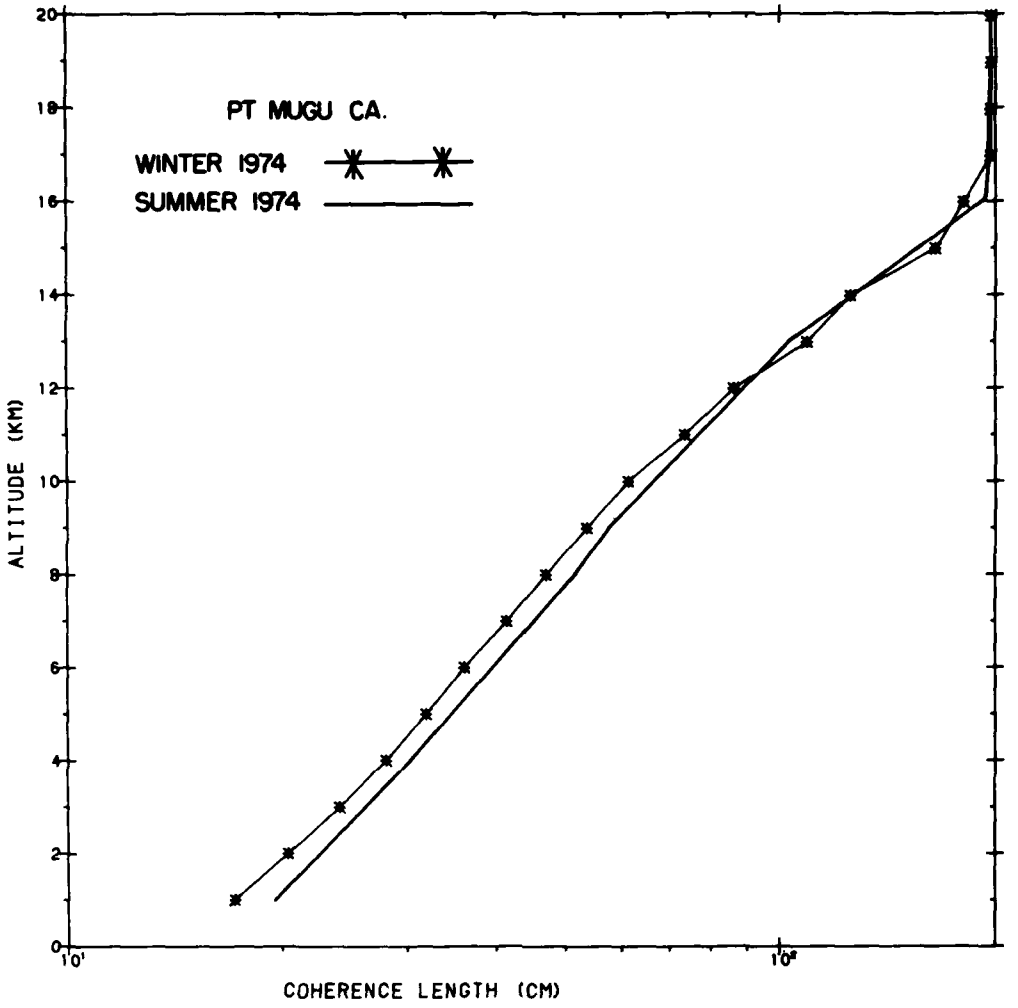

Figure 11. Coherence Length vs Altitude: Winter and Summer 1974, Pt. Mugu, Calif.

In many applications an accurate determination of r_0 above the first inversion layer may not be possible due to lack of data and/or may not be necessary due to the limited contribution of this region when compared to that of the region below. Walters and Kunkel[19] describe an approach used to estimate this contribution. We have integrated Hufnagel's model (Section 2) to evaluate I, obtaining:

$$I = 8.2 \times 10^{-23} u^2 f(z_0) e^{-z_0} + 4.05 \times 10^{-13} e^{(-z_0/1.5)} \quad (26)$$

where

$$f(z_o) = \sum_{i=0}^{10} \frac{10!}{i!} z_o^i . \qquad (27)$$

This should, for a proper choice of u, form a reasonable estimate of I for z_0 corresponding to heights above the first inversion layer.

Hufnagel[3] suggests that u is normally distributed and for Maryland has a mean of 27 m/sec with a standard deviation of 9 m/sec. In order to calculate r_o for conditions of high, moderate, and low turbulence, we have used the above expression for I with u = 36, 27, and 18 m/sec respectively. The results are shown in Figure 12. Although the graph is shown down to z_o = 1 km, it must be remembered that this model's validity does not begin until we are above the first inversion layer which may or may not be this low. A similar calculation can be done at other locations using the appropriate value of u.

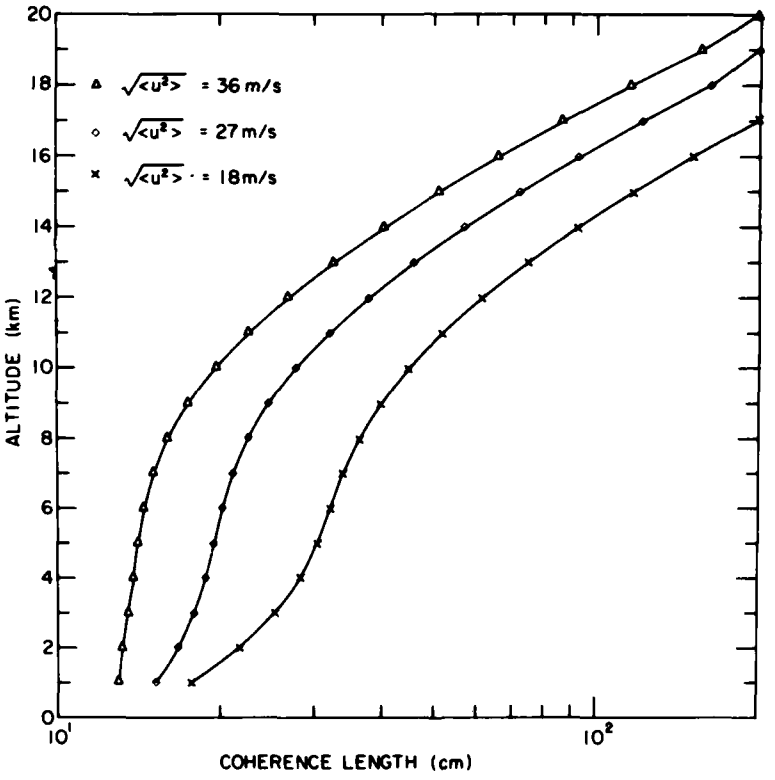

Figure 12. Coherence Length vs Altitude: for rms Wind Speeds of 18, 27, and 36 m/sec From Hufnagel Model

It has been suggested that we try to estimate the effects of the atmosphere below the first inversion layer in r_o through the use of Kaimal's model[20] as modified by Walters and Kunkel[19] and as has been done by Brown et al.[21] This unfortunately does not seem feasible using our data base since the rawinsonde data lacks the necessary resolution required to consistently determine the height of the first inversion layer.

In order to compare the above two methods, we must choose a method for determining a seasonal value of u to use in Hufnagel's model. At each kilometer level, from 5 to 20 km, for each launch we calculate the square of the velocity. We then choose the median for that level for the appropriate season. It is felt that because of the spread in values of wind speeds from launch to launch, the median is more representative than the mean. Then u is the rms value of these medians from 5 to 20 km.

Agreement between the two models is not particularly good. When u^2 lies in the range 150 to 275 m^2/sec^2 agreement is best (Figure 13). At higher values of u^2, Van Zandt's model yields a value of r_0 in excess of Hufnagel's model for the same value of z_0 (Figure 14) while at low wind speeds the reverse is true (Figure 15). The reason for this discrepancy is that Van Zandt's model is relatively insensitive to u^2 whereas for values of z and u^2 sufficiently large, Hufnagel's model predicts that C_n^2 should be directly proportional to this parameter. Figure 16 is a graph of C_n^2 versus z for Chatham, Mass. for the winter of 1974 and San Andres, Columbia for the spring of 1974. These two stations and seasons were chosen for comparison because they have the largest and smallest values of u^2 that we have encountered. 1258 m^2/sec^2 and 36.6 m^2/sec^2 respectively. We see little difference between the two, but Hufnagel's model predicts that they should differ by a factor of 34.

6. CONCLUSIONS

We have used Van Zandt's model of 1981[5] (with some modifications) in conjunction with the rawinsonde data base to calculate median values of C_n^2 at various stations for each season at each kilometer level from 1 km to 25 km. These results were examined statistically for seasonal and latitudinal variations. We have calculated the drop-off rate of C_n^2 (in dB/km) from 15 km to 25 km and the coherence length, r_0, for plane wave propagation down through the atmosphere. In addition, we used Hufnagel's model[1,3] to calculate r_0 from the same data base. We conclude that:

---

20. Kaimal, J.C. Wyngaard, J.C., Haughen, D.A., Cote, O.R., Izumi, Y.L., Caughey, S.J., and Readings, C.J. (1976) Turbulence structure in the convective boundary layer, J. Atm. Sci., 33:2152-2169.

21. Good, R.E., Brown, J.H., and Quesada, A.F. (1982) Measurement of high altitude resolution C_n^2 profiles and their importance on coherence lengths, Proceedings of SPIE, the Inter. Soc. for Opt. Eng. 365:105-111.

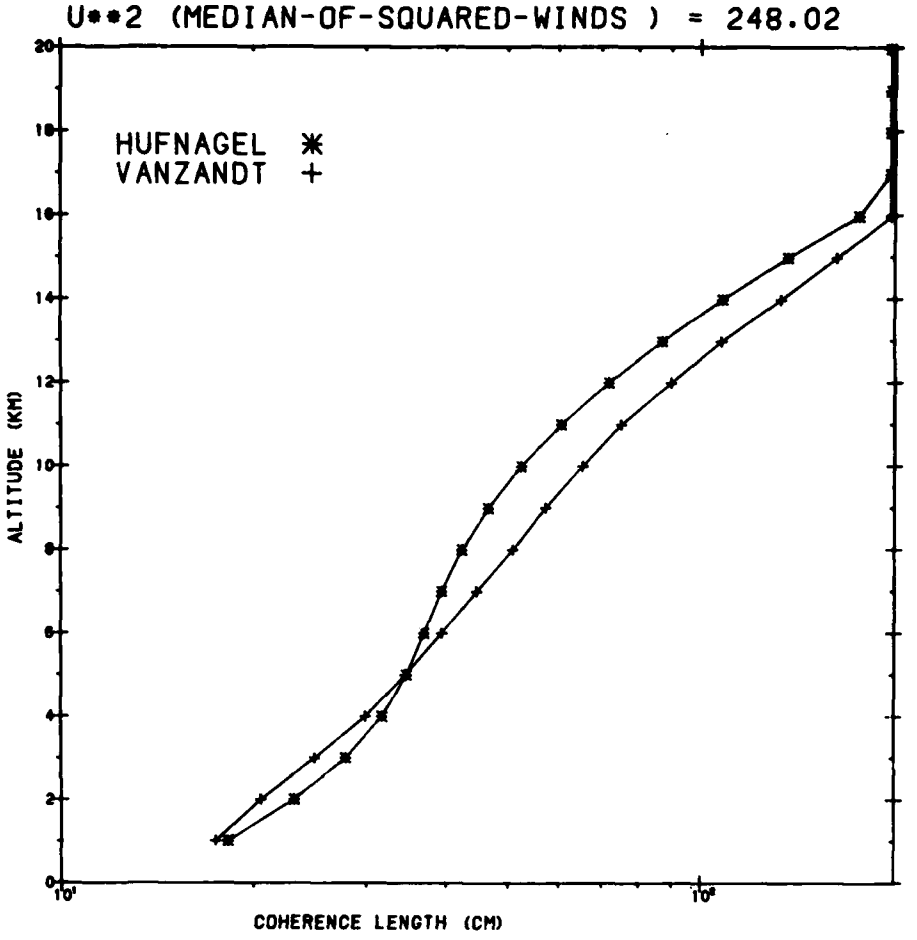

Figure 13. Coherence Length vs Altitude: Spring 1974, Pt. Mugu, Calif., From Van Zandt and Hufnagel Models

(1) There are statistically significant differences in median C_n^2 distributions, both latitudinally and seasonally. The four stations were broken up seasonally and the four stations were compared for each season. Each station was also examined separately and the four seasons were compared for each station.

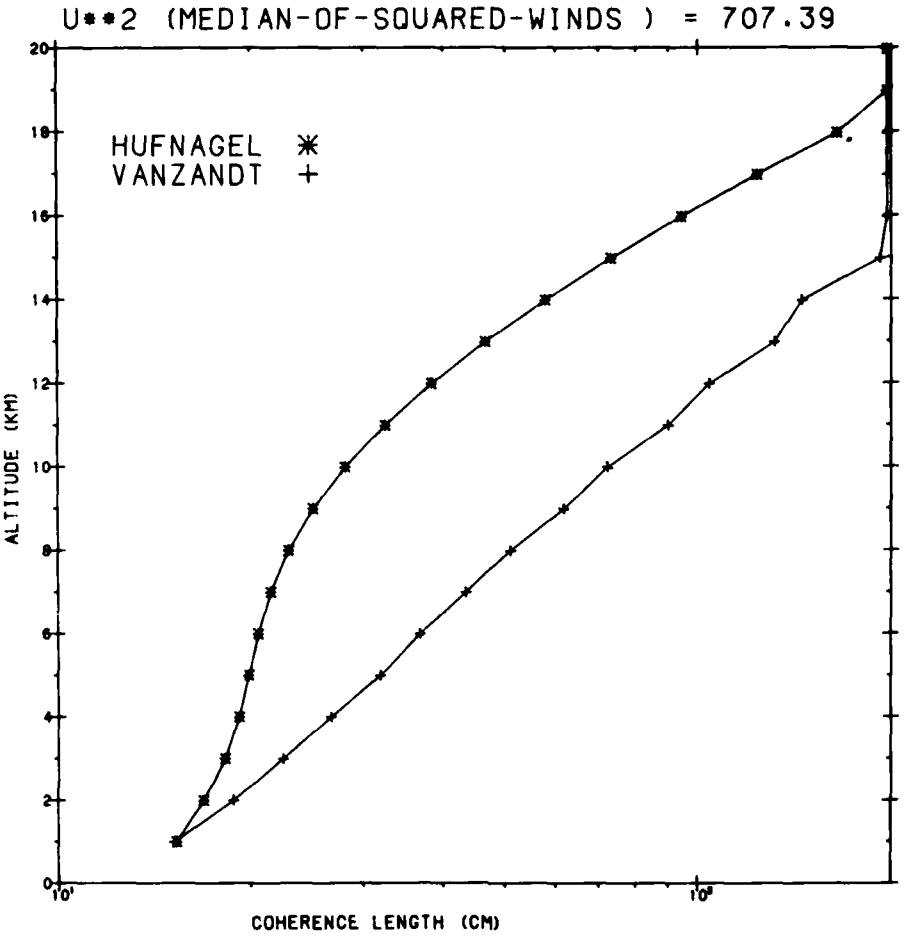

Figure 14. Coherence Length vs Altitude: Winter 1974, International Falls, Minn., From Van Zandt and Hufnagel Models

(2) The drop-off rate is a decreasing function of latitude, but varies only slightly with longitude and season. Seasonal values from Van Zandt's model are somewhat smaller than those obtained from radar at comparable latitudes. This is possibly due to the shorter time periods used in the radar results.

(3) Much of the drop-off rate can be explained as due to the decrease in density with altitude, 99 percent at 71° N and about 92.5 percent at 12° N.

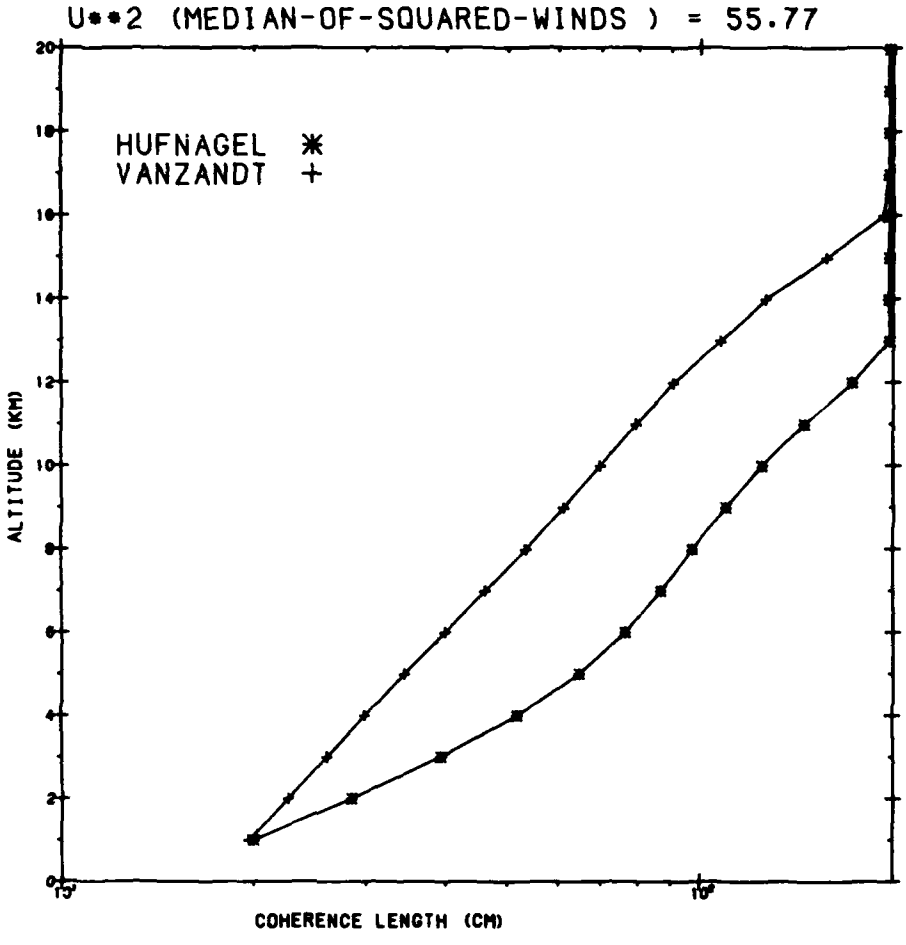

Figure 15. Coherence Length vs Altitude: Summer 1974, Brownsville, Tex., From Van Zandt and Hufnagel Models

(4) The coherence length for an optical plane wave can be calculated from Van Zandt's model and from Hufnagel's model. However, major discrepancies between the two models occur at very low and high wind speeds.

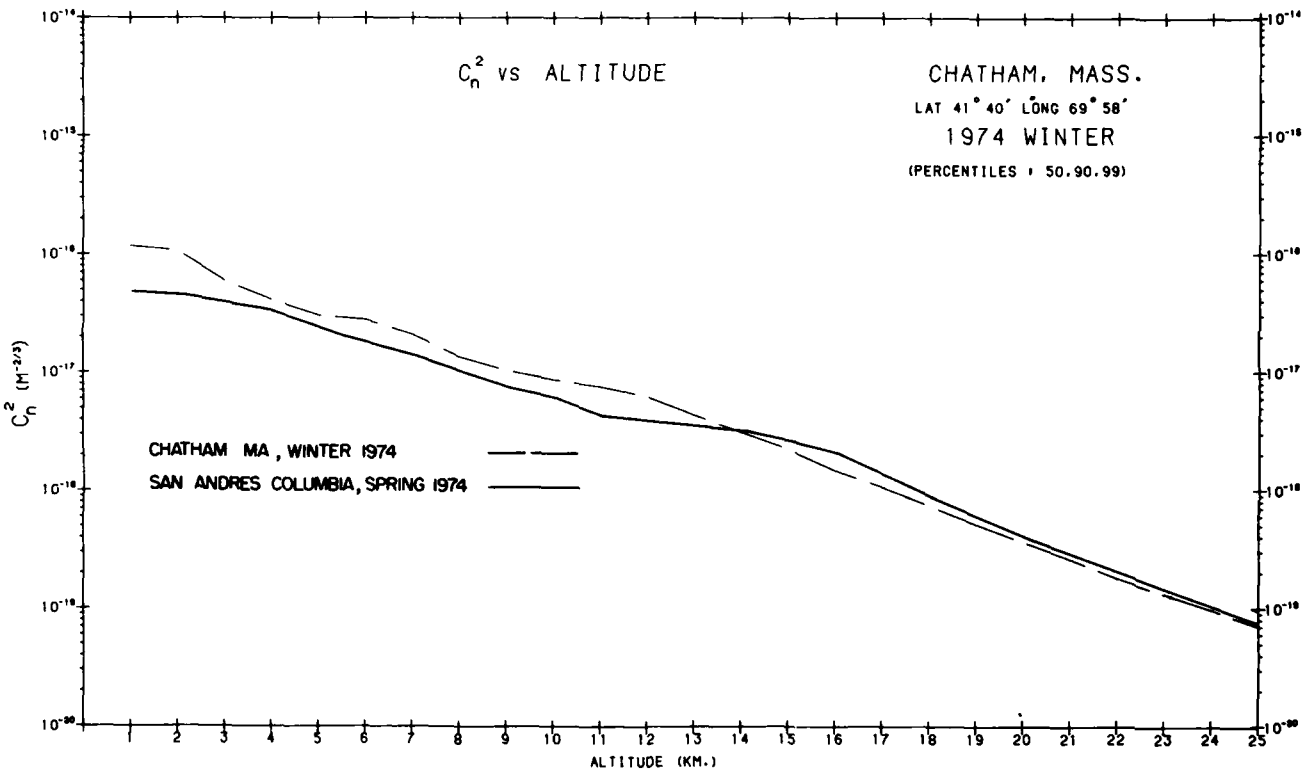

Figure 16. C_n^2 vs Altitude: Winter 1974, Chatham, Mass., and Spring 1974, San Andreas, Columbia

References

1. Hufnagel, R. E. (1978) Propagation through atmospheric turbulence, in The Infrared Handbook, U.S. Government Printing Office, Washington, D.C., Chap. 6, 6-1, 6-56.

2. Good, R. Earl, Watkins, B.J., Quesada, A.F., Brown, J.H., and Loriot, G.B. (1982) Radar and optical measurements of C_n^2, Appl. Opt. 21:3373-3376.

3. Hufnagel, R. E. (1974) Variations of atmospheric turbulence in Digest of Technical Papers, Topical Meeting on Optical Propagation Through Turbulence, Optical Society of America, WA 1-1, WA 1-4.

4. Van Zandt, T. E., Green, J. L., Gage, K. S., and Clark, W. L. (1978) Vertical profiles of refractivity turbulence structure constant: Comparison of observations by the Sunset radar with a new theoretical model. Radio Sci., 13:819-829.

5. Van Zandt, T. E., Gage, K. S., and Warnock, J. M. (1981) An improved model for the calculation of profiles of C_n^2 and ϵ in the free atmosphere from background profiles of wind, temperature and humidity, Preprints 20th Conf. Radar Meteorol. Soc., Boston; Amer. Meteor. Soc., pp 129-135.

6. Murphy, E. A., D'Agostino, R. E., and Noonan, J. P. (1982) Patterns in the occurrences of Richardson numbers less than unity in the lower atmosphere, J. Appl. Meteorol., 21:321-333.

7. Murphy, E., and Scharr, K. (1981) Modelling Turbulence in the Lower Atmosphere Using Richardson's Criteria, AFGL-TR-81-0349, AD A115244.

8. Balsley, B. B., and Peterson, V. L. (1981) Doppler radar measurements of clear air turbulence at 1290 MHz, J. Appl. Meteorol., 20:266-274.

9. Barletti, R., Cappatelli, G., Paterno, L., Righini, A., and Speroni, N. (1976) Mean vertical profile of atmospheric turbulence relevant for astronomical seeing, J. Opt. Soc. Am., 66:1380-1383.

10. Nastrom, G. D., Gage, K. S., and Balsley, B. B. (1982) Variability of C_n^2 at Poker Flat, Alaska, from mesosphere, stratosphere and troposphere (MST) Doppler radar observations, Opt. Eng., 21:347-351.

11. Tatarskii, V.I. (1971) The Effects of the Turbulent Atmosphere on Wave Propagation, U.S. Dept. of Commerce, National Technical Information Service, Springfield, VA, pp. 74-76.

12. Essenwanger, O. (1963) On the derivation of frequency distributions of vector wind shear values for small shear intervals, Geophysica Pura e Applicata, 56:216-224.

13. Van Zandt, T.E. (1983) private communication.

14. Weinstock, J. (1980) Vertical wind shears, turbulence, and non-turbulence in the troposphere and stratosphere, Geophys. Res. Letts., 7:749-752.

15. Good, R.E., Quesada, A.F., Brown, J.H., and Dewan, E.M. (1984) Probability distribution of turbulence layer thickness in the stratosphere, J. Geophys. Res., to be published.

16. Dixon, W.J., and Massey, F.J. (1969) An Introduction to Statistical Analysis, McGraw-Hill, p. 351.

17. Fried, D.L., and Meyers, G.E. (1974) Evaluation of r_o for propagation down through the atmosphere, Appl. Opt., 13:2620-2622.

18. Gracheva, M., and Gurvich, A. (1980) A simple model for calculation of turbulence noise in optical systems, Atmospheric and Oceanic Physics, 16:819-822.

19. Walters, D.L., and Kunkel, K.E. (1981) Atmospheric transfer function for desert and mountain locations: the atmospheric effects on r_o, J. Opt. Soc. Am., 71:397-405.

20. Kaimal, J.C., Wyngaard, J.C., Haugen, D.A., Cote, O.R., Izumi, Y.L., Caughey, S.J., and Readings, C.J. (1976) Turbulence structure in the convective boundary layer, J. Atm. Sci., 33:2152-2169.

21. Good, R.E., Brown, J.H., and Quesada, A.F. (1982) Measurement of high altitude resolution C_n^2 profiles and their importance on coherence lengths, Proceedings of SPIE, the Inter. Soc. for Opt. Eng. 365:105-111.

Appendix A

A Subroutine to Calculate $C_n^2(P/T)^2$ for Van Zandt's Model for $N > 0$

```
      SUBROUTINE VZCNSQ(NBAR,SBAR,CN2)
      DIMENSION L(19),N(1000),S(1000)
      DIMENSION PS(1000),PN(1000)
      REAL L,NBAR,N,MMBSI0
      DATA L/0.2,0.4,0.6,0.8,1.0,2.0,3.0,4.0,6.0,10.,20.,40.,60.,80.,
     X100.,200.,400.,600.,800./
C     FUNCTIONS
C     C3 REPRESENTS THE THICKNESS, L
C     A REPRESENTS THE STABILITY, N
C     ALL DIMENSIONS MUST BE IN M,K,S,  SYSTEM
C     SBAR REPRESENTS THE AVERAGE SHEAR SQUARED
C     M=-A P/T N/G
C     6.266E-11 = (A/G)**2
C     CN IS REALLY CN (T/P)
C     CN IS FOR DRY CONDITONS
C
C
C -----  HERE DEFINE LOCAL FUNCTIONS SIGMAS AND CNSQ
      SIGMAS(ABAR,C3)=0.2*ABAR**0.25*(C3)**(-0.3)
      CNSQ(A,C3)=2.8*C3**(1.3333)*(6.266E-11)*A*A
C
      SQRT2PI=SQRT(2.0*3.14159)
      RI=0.25
      SUM=0.0
      NCNT=20
      TSTART=-3.
      SQRTSBA=SQRT(SBAR)
      DO 40 KL=7,14
C     THIS LOOP INTEGRATES OVER THE VARIOUS SPECIFIED LAYER THICKNESS
C
      PL=0.01
      IF(KL.EQ.1) THEN
      DEL=0.2
      GO TO 6
      END IF
      DEL=L(KL)-L(KL-1)
C
    6 SIG=SIGMAS(NBAR,L(KL))
      SIGSQ=SIG*SIG
      SIGMAN=SIG*SQRT(NBAR)
C
      SUMN=0.0
      DO 30 I=1,NCNT
C     THIS LOOP INTEGRATES OVER THE STABILITY PARAMETER 'N'
C
      IF(I.NE.1) GO TO 14
```

```
      DELT=-2.0*TSTART/NCNT
      DELN=DELT*SIGMAN
      T=TSTART
      N(I)=T*SIGMAN+NBAR
      GO TO 15
   14 T=T+DELT
      IF(T.GT.-TSTART) GO TO 31
      N(I)=T*SIGMAN+NBAR
   15 C2=T*T/2
      IF(N(I).LT.-.0004) GO TO 30
      CN=CNSQ(N(I),L(KL))
      IF(C2.GT.100.) THEN
      PN(I)=0.0
      GO TO 30
      ELSE
      PN(I)=EXP(-C2)/SQRT2PI/SIGMAN
      END IF
      SUMS=1.0E-30
      DO 20 J=1,NCNT
C     THIS LOOP IS OVER THE S VARIABLE
C
      IF(J.NE.1) GO TO 17
      S(1)=N(I)/RI
      IF(N(I).LE.0.0) S(1)=1.0E-8
      TT=(SQRT(S(1))-SQRTSBA)/SIG
      DELTT=-2.0*TSTART/NCNT
      C2=2.0*SIG*DELTT
      R=N(I)/S(J)
      GO TO 18
   17 TT=TT+DELTT
      S(J)=(SIG*TT+SQRTSBA)**2
      R=N(I)/S(J)
      IF(TT.GT.-TSTART.AND.R.LT.0.05) GO TO 21
   18 IF(R.GT.25) GO TO 20
      DELS=ABS(C2*(SIG*TT+SQRTSBA))
      SS=SQRT(S(J)*SBAR)/SIGSQ
C     IF(SS.GT.475.) GO TO 20
      C1=(SQRT(S(J))-SQRTSBA)**2/(2.0*SIGSQ)
      IF(C1.GT.100.) THEN
      PS(J)=0.0
      GO TO 20
      ELSE
      BESSEL=MMBSI0(2,SS,IER)
C     THE ARGUMENT 2 REPRESENTS   EXP(-SS) I(SS)
      PS(J)=EXP(-C1)*BESSEL/(2.0*SIGSQ)
      END IF
      SUMSS=PS(J)*PL*CN*PN(I)*DELS*DELN*DEL
      SUMS=SUMS+SUMSS
C     IF(N(I).GE.0.0.AND.SUMSS/SUMS.LT.0.001) GO TO 21
   20 CONTINUE
   21 SUMN=SUMN+SUMS
```

```
C     IF(SUMS/SUMN.LT.0.001) GO TO 31
 30   CONTINUE
 31   SUM=SUM+SUMN
      IF(SUMN/SUM.LT.0.001) GO TO 41
 40   CONTINUE
 41   CN2=SUM
      RETURN
 999  FORMAT(10X,3HKL=,I4,8G15.3)
 998  FORMAT(8X,3H I=,I4,8G15.3)
 997  FORMAT(2X,3H J=,I4,8G14.3)
 996  FORMAT(20X,'SBAR AND NBAR =  ',G15.4,2X,G15.6)
 995  FORMAT(20X,' CN SQ =',G15.4)
 994  FORMAT(A6)
 993  FORMAT(1H1)
 992  FORMAT(10X,20H TSTART AND NCNT =  ,F6.0,I5)
      END

COMMAND-
```

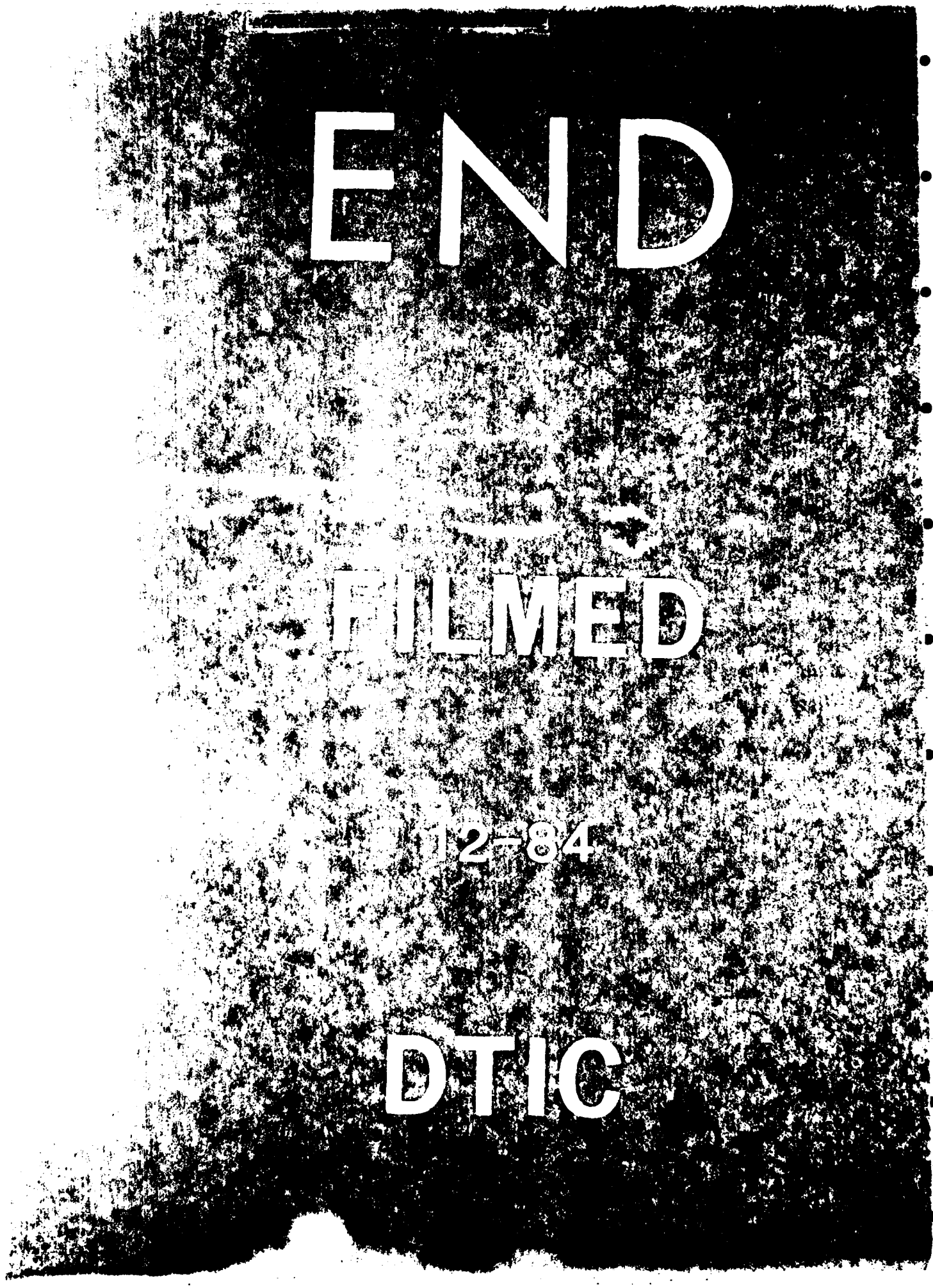
END
FILMED
12-84
DTIC